PHYSICAL REVIEW C **93**, 024301 (2016)

High-precision γ-ray spectroscopy of the cardiac PET imaging isotope ^{82}Rb and its impact on dosimetry

M. N. Nino,[1] E. A. McCutchan,[2] S. V. Smith,[3] C. J. Lister,[4] J. P. Greene,[5] M. P. Carpenter,[5] L. Muench,[3] A. A. Sonzogni,[2] and S. Zhu[5]

[1]*Department of Physics and Astronomy, Hofstra University, Hempstead, New York 11549, USA*
[2]*National Nuclear Data Center, Brookhaven National Laboratory, Upton, New York 11973, USA*
[3]*Collider Accelerator Department, Brookhaven National Laboratory, Upton, New York 11973, USA*
[4]*Department of Physics and Applied Physics, University of Massachusetts Lowell, Lowell, Massachusetts 01854, USA*
[5]*Physics Division, Argonne National Laboratory, Argonne, Illinois 60439, USA*

(Received 2 October 2015; revised manuscript received 21 December 2015; published 1 February 2016)

^{82}Rb is a positron-emitting isotope used in cardiac positron emission tomography (PET) imaging which has been reported to deliver a significantly lower effective radiation dose than analogous imaging isotopes like ^{201}Tl and ^{99m}Tc sestamibi. High-quality β-decay data are essential to accurately appraise the total dose received by the patients. A source of ^{82}Sr was produced at the Brookhaven Linac Isotope Producer (BLIP), transported to Argonne National Laboratory, and studied with the Gammasphere facility. Significant revisions have been made to the level scheme of ^{82}Kr including 12 new levels, 50 new γ-ray transitions, and the determination of many new spin assignments through angular correlations. These new high-quality data allow a precise reappraisal of the β-decay strength function and thus the consequent dose received by patients.

DOI: 10.1103/PhysRevC.93.024301

I. INTRODUCTION

Cardiovascular disease is the leading cause of death in most countries. A number of agents like ^{13}N-ammonia, ^{15}O-water, ^{82}Rb, ^{99m}Tc sestamibi/tetrofosmin, and ^{201}Tl have been developed for the diagnosis and management of patients with ischemic heart disease by myocardial perfusion imaging (MPI). However, ^{82}Rb is rapidly becoming the agent of choice for cardiac positron emission tomography (PET) imaging in the USA, Europe, and Asia [1]. This is due to the fact that ^{82}Rb has higher accuracy when compared to the single-photon emission computed tomography (SPECT) imaging agents [2], has a short half-life ($T_{1/2} = 76$ s), and delivers a lower dose compared with ^{201}Tl and ^{99m}Tc agents [3].

As the number of noninvasive PET imaging procedures increases, the exact radiation exposure becomes a concern. There are currently significant discrepancies in estimates of the absorbed dose from ^{82}Rb treatment [4]. A recent study [5] finds the effective dose is four times lower than that recommended by the International Commission on Radiological Protection (ICRP) [6]. There are two components involved in calculating the absorbed dose: a nuclear physics component factoring in the relevant properties of the decay (half-life, γ and β energies and intensities) and a kinetic component which involves exactly how the radiation is transported and cataloged in the different tissues and organs. The former can be directly and precisely measured, as is done in the present study, while the latter requires a theoretical model and Monte Carlo simulations [7].

For PET imaging, the only radiation of interest is the back-to-back 511-keV γ rays from stopped positron annihilation so the ideal source would only provide this decay mode. No source can have this property; in the leptonic sector, positron β decay always competes with electron capture (EC), the positrons have considerable kinetic energy, and the decay is seldom purely ground state to ground state, while in the annihilation sector the positrons can decay in flight or can decay into three or more photons. The total γ-ray emission per decay in a perfect PET source would be 1022 keV, and the total electron kinetic energy would be zero. Deviations from these ideal numbers can be used to quantify any potential positron emitter and be used to estimate the added dose delivered by these undesirable decay paths. In this specific case of ^{82}Rb, $\sim$85% of the decay proceeds to the krypton ground state and $\sim$15% to the first excited state at 776.5 keV, so the mean total γ-ray emission is raised to $\sim$1138 keV. The issue in question here is quantifying the additional contribution from all other excited states populated in the decay. With a Q value of over 4 MeV, the highly fragmented flux to very high-lying states, which frequently is missed in low-sensitivity, high-resolution γ-ray spectroscopy [8], could significantly add to the γ-ray burden.

The full decay scheme of ^{82}Rb was last studied in 1983 by Meyer *et al.* [9] using small Ge(Li) detectors and an analysis which relied mainly on so-called singles data. While γ-γ coincidence data were recorded, these data were only viable for the strongest transitions in the decay due to poor counting efficiency (see Fig. 2(c) of Ref. [9]). The proper identification of all the γ-ray transitions and their correct placement in the decay scheme is particularly important, since the β-feeding pattern is not directly measured but inferred from balancing the γ-ray population and decay at each excited level. In order to ensure that the nuclear physics component of dose calculations for ^{82}Rb has a more solid basis, we have revisited the decay of ^{82}Rb using the state-of-the-art, Compton-suppressed Gammasphere array.

While the full γ-ray decay scheme was last studied more than 30 years ago, the intensity of the 776.5-keV, $2_1^+ \rightarrow 0_1^+$ transition in ^{82}Kr as a fraction of ^{82}Rb decays has been more carefully investigated in several studies. Two previous

 ©2016 American Physical Society

measurements performed in 1987 found the absolute intensity for the 776.5-keV transition to be 0.1512(18) [10] and 0.149(4) [11]. A newer measurement [12] from 2012 yielded a value of 0.1493(37). This precise and consistent value of the absolute intensity of the 776.5-keV transition provides a solid basis to absolutely normalize the current decay scheme. From this, we can extract a reliable β-feeding distribution and consequently allow a better quantification of the actual dose received.

II. EXPERIMENT

A source of ^{82}Sr was produced by irradiating thick RbCl targets with protons for 3 weeks at the Brookhaven Linear Isotope Producer (BLIP). The target was sufficiently thick that the proton beam covered an energy range from 100 to 40 MeV. The RbCl puck was dissolved in a strong ammonium chloride solution and the ^{82}Sr was chemically separated using a series of ion exchange columns as described in Refs. [13,14]. The isolated, carrier-free ^{82}Sr ($T_{1/2} = 25.35$ days) is the parent of the daughter ^{82}Rb and supplied in generator form for delivery of ^{82}Rb to the clinical site. Approximately 100 μCi of ^{82}Sr was shipped to Argonne National Laboratory for analysis using Gammasphere. In this experiment, Gammasphere [15] consisted of 89 Compton-suppressed HPGe detectors. Gammasphere was operated with constant fraction timing. The source was counted for 7 days with a γ-ray so-called singles trigger and for 4 days with a hardware 1.5-μs γ-γ coincidence window. In total, there were 2.2×10^{10} singles events recorded and 1.9×10^{9} coincidence events containing two γ-rays or more. Figure 1 illustrates the quality of these data.

There are two β decaying states in ^{82}Rb, the short-lived ($T_{1/2} = 76$ s) ground state with $J^{\pi} = 1^{+}$ and a 68.9-keV longer-lived ($T_{1/2} = 6.47$ h) isomer with $J^{\pi} = 5^{-}$ [16]. The source of our ^{82}Rb is from the decay of the ^{82}Sr parent, which due to its $J^{\pi} = 0^{+}$ ground state and low Q value of only 180 keV, is expected to populate only the $J^{\pi} = 1^{+}$ ground state of ^{82}Rb. We expect the 5^{-} isomer not to be directly populated, as the decay would correspond to a highly hindered, fifth forbidden transition. We confirm this in our γ-γ analysis as described in Sec. IV A.

III. DATA ANALYSIS

Data were sorted using the GSSORT [17] package to construct both γ-ray singles spectra and γ-γ coincidence matrices. A 50-ns time coincidence requirement was placed for the construction of the γ-γ coincidence matrix. The analysis was performed using a modified version of the Radware package GF3 [18].

Calibration of the efficiency of the Gammasphere array followed the procedure described in Ref. [19] using very well-known transitions in the decay of ^{182}Ta [20] and ^{56}Co [21]. The intensities reported here include a 2% systematic uncertainty on efficiency for $E_{\gamma} < 1$ MeV and 5% for energies larger than 1 MeV.

In general, intensities were determined using gates from below, as described in Ref. [19]. As the lowest energy transition is ~400 keV, no corrections were necessary for low-energy walk or jitter. When possible, branching ratios out of a level were confirmed using a gate on a transition feeding into the level. There are a large number of ground-state transitions in the decay of ^{82}Rb. The transitions of 1475 and 1957 keV could be determined using gates from above and relative branching ratios out of the level. The remainder of the ground-state transitions had to be determined from the singles data.

Angular correlations were performed to determine level spins and transition multipolarities. The detectors that compose Gammasphere were separated into 16 angle groups for this analysis. The average angle values for these angle groups are as follows: 20.3°, 34.8°, 40.6°, 53.2°, 60.7°, 71.5°, 80.4°, 90°, 99.6°, 108.6°, 119.3°, 126.8°, 139.4°, 145.1°, 159.7°, and 180°. Efficiency of each angle bin was determined by first determining the individual efficiency of each Gammasphere detector and then taking the sum of the product of each of the detector pairs in each bin. There were sufficient statistics that the 0–90° and 90–180° groups could be analyzed independently. In cases where the mixing ratio, δ, could be determined the final quoted result is a weighted average of the 0–90° and 90–180° analysis.

IV. EXPERIMENTAL RESULTS

Table I lists the energies and intensities of the γ rays observed in this analysis and assigned to the decay of ^{82}Rb. The

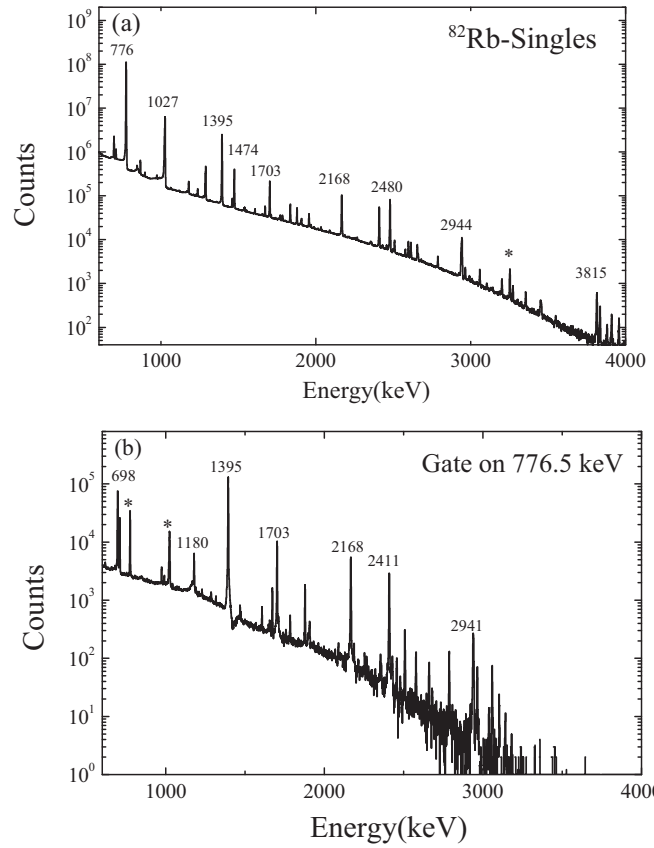

FIG. 1. (a) Singles spectrum from the decay of ^{82}Rb. (b) Spectrum obtained by gating on the 776-keV transition in ^{82}Kr. In both panels, strong transitions belonging to the decay of ^{82}Rb are labeled by their energy in keV, while background lines are indicated with a *.

TABLE I. Levels populated in ^{82}Kr and their γ decay. Relative intensities for the depopulating γ-ray transitions are given by I_γ. The I_γ's are normalized to $2_1^+ \rightarrow 0^+_1 \equiv 100$. The I_γ's are also compared with literature values [9] where available. δ values were obtained where statistics were sufficient.

J_i^π	E_i (keV)	J_f^π	E_f (keV)	E_γ (keV)	I_γ	δ	I_γ^{lit}([9])
2^+	776.53(7)	0^+	0.00	776.53(7)	100(2)		100
2^+	1474.89(7)	2^+	776.53	698.32(7)	0.95(3)		0.99(3)
		0^+	0.00	1474.93(7)	0.63(2)		0.59(2)
0^+	1487.62(10)	2^+	776.53	711.09(7)	0.358(8)		0.38(2)
4^+	1820.35(19)	2^+	776.53	1044.12(18)	0.008(1)		0.006(4)
2^+	1956.91(8)	2^+	776.53	1180.31(7)	0.112(6)	-0.52 ± 0.16	0.11(1)
		0^+	0.00	1956.97(7)	0.043(2)		0.045(4)
3^+	2094.18(15)[a]	2^+	1474.89	619.16(13)[b]	0.0103(8)		
		2^+	776.53	1317.77(13)[b]	0.0063(7)		
0^+	2171.77(10)	2^+	1474.89	696.85(7)	0.176(4)		0.51(2)
		2^+	776.53	1395.26(7)	3.81(19)		3.51(2)
0^+[c]	2450.17(10)	2^+	1474.89	975.22(7)	0.056(2)		0.056(7)
		2^+	776.53	1673.70(7)[b]	0.045(3)		0.047(3)
2^+[c]	2480.00(15)	2^+	1956.91	523.24(7)	0.062(2)		0.03(1)
		4^+	1820.35	659.38(7)[b]	0.0050(3)		
		2^+	1474.89	992.27(9)	0.0139(4)		0.012(5)
		2^+	776.53	1703.54(7)	0.36(2)	1.03 ± 0.10	0.335(4)
		0^+	0.00	2480.23(7)	0.24(1)		0.27(1)
(3^-)	2547.38(11)[a]	2^+	1474.89	1072.49(8)[b]	0.0081(7)		
2^+[c]	2655.98(16)	2^+	1956.91	699.41(13)[b]	0.0042(6)		
		0^+	1487.62	1168.23(7)	0.0060(3)		0.009(4)
		2^+	1474.89	1181.05(7)	0.0091(8)		0.02(1)
		2^+	776.53	1879.61(7)	0.068(4)	-0.71 ± 0.21	0.067(4)
		0^+	0.00	2655.56(8)	0.0141(3)		0.017(4)
	2676.03(21)[a]	2^+	776.53	1899.5(3)[b]	0.0069(9)		
	2684.43(14)[a]	2^+	776.53	1907.90(12)[b]	0.018(1)		
2[c]	2944.56(10)	(3^-)	2547.38	396.93(20)[b]	0.0029(5)		
		3^+	2094.18	850.37(7)[b]	0.0026(2)		
		2^+	1956.93	987.60(21)[b]	0.0031(5)		
		2^+	1474.89	1469.64(9)[b]	0.016(1)		
		2^+	776.53	2168.06(7)	0.262(13)	< 0.06	0.28(1)
		0^+	0.00	2944.61(12)	0.0358(18)		0.05(1)
	2964.79(17)[a]	2^+	776.53	2188.26(16)[b]	0.0037(7)		
	2993.23(31)[a]	2^+	776.53	2217.7(3)[b]	0.0010(4)		
		0^+	0.00	2992.97(21)[b]	0.0017(2)		
	3131.31(23)[a]	2^+	1474.89	1656.47(22)[b]	0.0021(5)		
		2^+	776.53	2354.73(24)[b]	0.0035(7)		
0^+[c]	3187.16(11)	2^+	1956.91	1230.35(7)[b]	0.0134(7)		
		2^+	1474.89	1712.24(7)	0.013(1)		0.011(2)
		2^+	776.53	2410.65(17)	0.165(8)		0.156(8)
	3207.03(31)[a]	2^+	776.53	2430.5(3)[b]	0.0032(5)		
	3217.12(31)[a]	2^+	1474.89	1742.23(30)[b]	0.0027(5)		
0^+[c]	3234.15(17)[a]	2^+	2480.00	754.03(16)[b]	0.0050(6)		
		2^+	1956.93	1276.93(19)[b]	0.0048(8)		
		2^+	776.53	2457.69(15)[b]	0.0050(5)		
	3285.79(23)[a]	2^+	2480.00	805.76(7)[b]	0.0043(4)		
		0^+	2171.77	1113.71(15)[b]	0.0007(2)		
		3^+	2094.18	1191.61(18)[b]	0.0048(3)		
		2^+	776.53	2509.31(7)[d]	0.0171(9)		0.019(5)

TABLE I. (*Continued*.)

J_i^π	E_i (keV)	J_f^π	E_f (keV)	E_γ (keV)	I_γ	δ	I_γ^{lit}([9])
$1,2^{(+)}$	3355.82(40)	2^+	1956.91	1399.31(23)[b]	0.0010(2)		
		2^+	776.53	2579.18(11)	0.0063(5)		0.0070(7)
		0^+	0.00	3356.09(10)	0.0019(1)		0.0019(2)
	3438.11(16)[a]	2^+	1474.89	1963.21(20)[b]	0.0020(5)		
		2^+	776.53	2661.58(14)[b]	0.0046(4)		
$1,2^{(+)}$	3458.03(41)	2^+	776.53	2681.5(4)[b]	0.0019(4)		
		0^+	0.00	3457.03(14)	0.00089(5)		0.00074(15)
0^+[c]	3565.23(11)	$1,2^{(+)}$	2655.98	908.85(22)[b]	0.004(1)		
		$1^+,2^+$	2480.00	1085.08(11)[d]	0.0032(4)		
		2^+	1956.91	1608.21(7)	0.0194(10)		0.015(2)
		2^+	1474.89	2090.00(29)[b]	0.0044(7)		
		2^+	776.53	2788.81(9)	0.0071(5)		0.0076(5)
0^+[c]	3716.57(8)	(3^-)	2547.38	1168.40(8)[d]	0.0032(2)		
		3^+	2094.18	1621.99(13)[b]	0.0020(2)		
		2^+	1956.91	1759.25(25)[b]	0.0026(4)		
		2^+	776.53	2940.69(10)	0.027(1)		0.021(4)
	3742.85(11)	(3^-)	2547.38	1195.72(16)[b]	0.0010(1)		
		0^+	2171.77	1570.88(15)[b]	0.0014(2)		
		3^+	2094.18	1648.76(23)[b]	0.0022(3)		
		2^+	1956.91	1785.85(7)	0.018(1)		0.020(4)
		0^+	1487.62	2255.02(31)[b]	0.0026(3)		
		2^+	1474.89	2268.24(21)[b]	0.0041(7)		
		2^+	776.53	2966.17(14)	0.0042(4)		0.0040(3)
$1,2^{(+)}$	3814.83(41)	2^+	776.53	3038.3(4)[b]	0.0009(2)		
		0^+	0.00	3815.15(7)	0.0036(1)		0.0030(2)
1,2	3835.94(14)	3^+	2094.18	1741.73(18)[b]	0.0039(3)		
		2^+	1474.89	2360.96(21)[b]	0.0042(7)		
		2^+	776.53	3059.47(12)	0.0053(4)		0.0045(3)
		0^+	0.00	3836.18(8)	0.00141(8)		0.00146(15)
$1,2^{(+)}$	3880.96(18)	$1^+,2^+$	2480.00	1400.82(10)[b]	0.0039(5)		
		3^+	2094.18	1786.7(3)[b]	0.0017(2)		
		2^+	1474.89	2405.95(13)[b]	0.0009(2)		
		2^+	776.53	3104.60(23)	0.0014(2)		0.0010(3)
		0^+	0.00	3881.47(19)	0.00041(5)		0.00058(14)
$1,2^{(+)}$	3910.75(12)	0^+	0.00	3910.75(12)	0.00095(7)		0.0007(1)
	3919.95(25)[a]	2^+	776.53	3143.42(24)[b]	0.0004(1)		
$1,2^{(+)}$	3957.95(14)	0^+	0.00	3957.95(14)	0.00081(6)		0.0006(1)

[a]Newly observed level populated in the β decay of ^{82}Rb.
[b]Newly observed γ-ray transition in the β decay of ^{82}Rb.
[c]New spin assignment based on angular correlation measurements.
[d]Placement differs from that proposed in Ref. [9].

intensities in the table have been normalized to the 776-keV, $2_1{}^+ \rightarrow 0_1{}^+$ transition in the decay of ^{82}Rb to ^{82}Kr, taking $I_{776} \equiv 100$. The level scheme is given in Fig. 2.

A. Discussion of levels

The high coincidence efficiency of Gammasphere allows for the identification and proper placement of numerous weak transitions feeding the high-lying states. As an example, the 1957-keV level was previously proposed [9] to be populated by just two tentatively placed transitions of 523 and 1786 keV and a firmly placed 1608-keV transition. In Fig. 3, a gate on the 1957-keV transition displays the observed transitions feeding into the 1957-keV level. The tentative 523-keV transition is confirmed and an accurate value of its intensity could be determined from the coincidence gate. The placements of the 1608- and 1786-keV transitions are also confirmed, along with the observation of 6 new transitions of 699, 988, 1230, 1277, 1399, and 1759 keV, all now placed as feeding into the 1957-keV level.

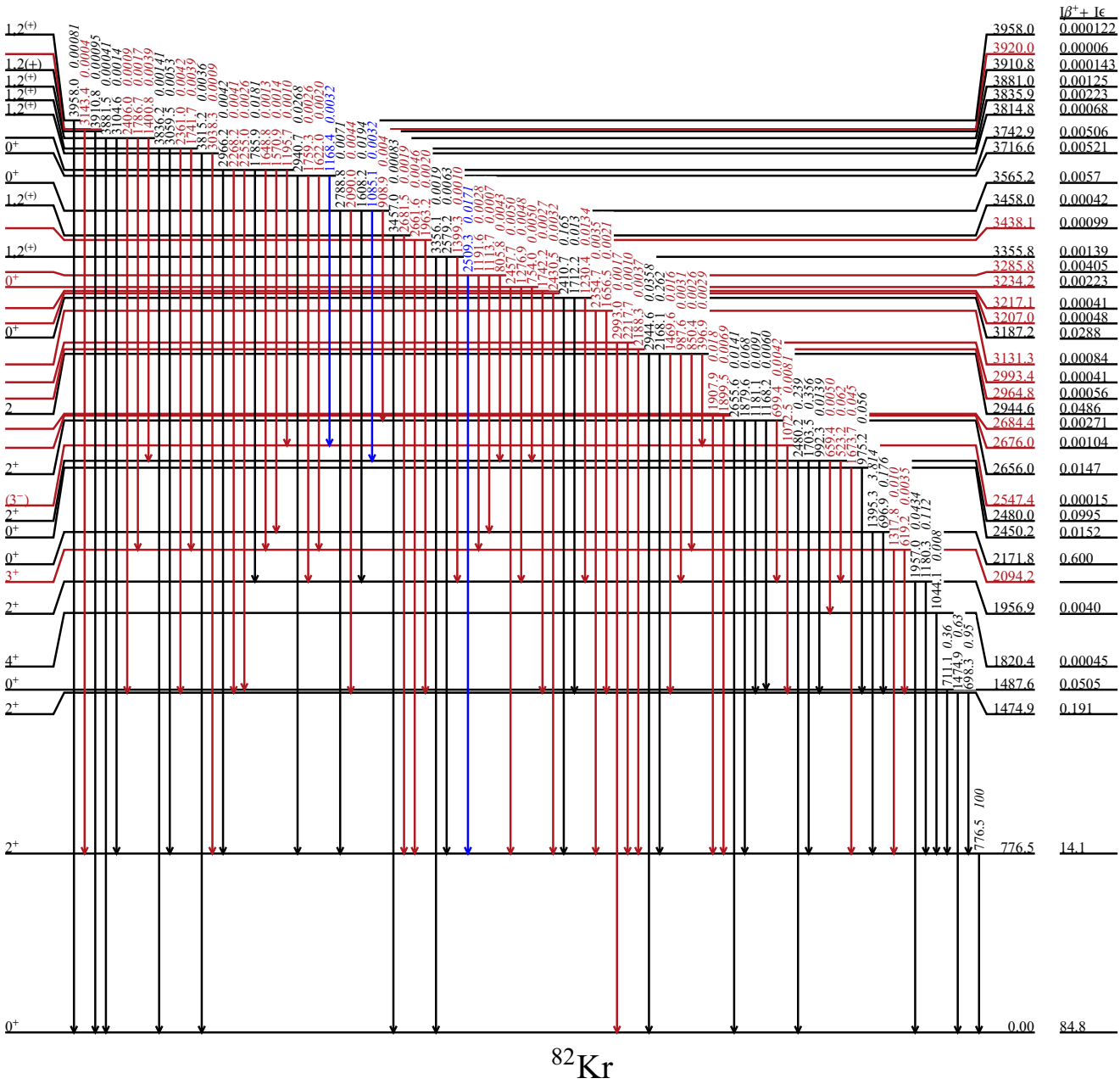

FIG. 2. Level scheme for ^{82}Kr based on the decay of ^{82}Rb. The energy levels are given in keV. Transition energies (in keV) are followed by the intensity in italics. $I_\beta^+ + I_\epsilon$ represents the total deduced β feeding for each level. Black lines indicate levels and transitions confirmed in the present work. Red lines indicate levels and transitions newly identified in the present work, while blue lines give transitions which were given new placements in the level scheme.

A level at 2094 keV is observed to decay to the 2_1^+ and 2_2^+ states through 1317- and 619-keV transitions, respectively, each of which are new to the β-decay scheme. Another level at 2547 keV is observed to decay to the 2_2^+ level through a new transition of 1072 keV. Both the 2094- and 2547-keV levels have been previously observed in other reactions and assigned as $J^\pi = 3^+$ and (3^-) levels, respectively [16]. Support for the first observation of the (3^-), 2547-keV level in the β^+ decay of ^{82}Rb is given in Fig. 4. In a gate on the 1072-keV transition, the strong transitions of 698, 776, and 1475 keV provide good evidence for the 1072-keV transition as populating the 2_2^+ level. In addition, two transitions are observed to feed into the (3^-), 2547-keV level, as shown in Fig. 4: one a new transition and the other placed in an alternate location in the level scheme by Ref. [9]. The 1168-keV transition was previously proposed to depopulate the 2656-keV level and feed into the 1488-keV level. The 1196-keV transition is a new transition into the 2547-keV level from the previously established 3743-keV level. There were also a number of new transitions observed to feed into the 3^+, 2094-keV level, as shown in Fig. 5 in a

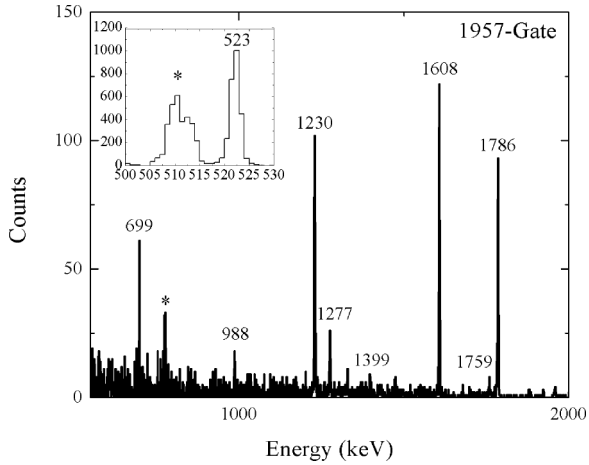

FIG. 3. Spectrum obtained by gating on the 1957-keV transition in ^{82}Kr illustrating transitions populating the 1957-keV level.

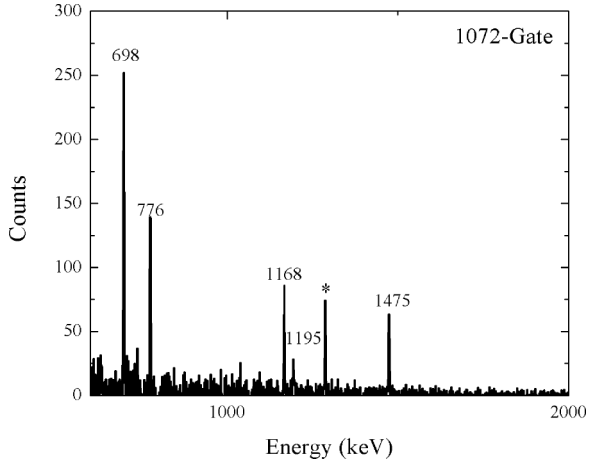

FIG. 4. Spectrum obtained by gating on the 1072-keV transition in ^{82}Kr, providing evidence for its placement depopulating a newly observed 2547-keV level.

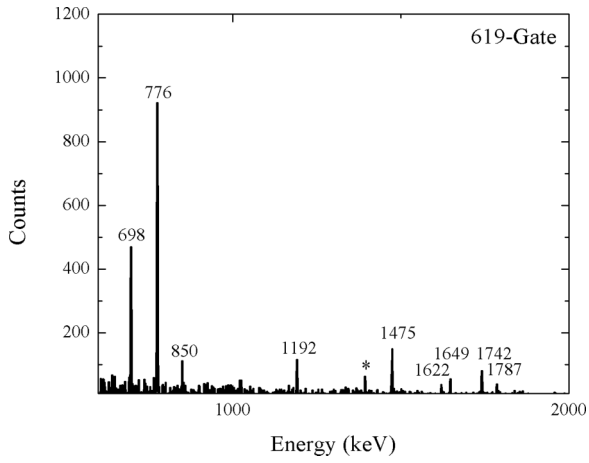

FIG. 5. Spectrum obtained by gating on the 619-keV transition in ^{82}Kr, providing evidence for its placement depopulating a newly observed 2094-keV level.

gate on the 619-keV transition. The new transitions feeding into this level are the 850-, 1192-, 1622-, 1649-, 1742-, and 1787-keV transitions.

The 2094-keV (3^+) and 2547-keV (3^-) levels have been previously observed in the β decay of the 6.47-h, 5^- isomeric level in ^{82}Rb [9]. To confirm that the levels observed in the present experiment were indeed populated in the decay of the ground state of ^{82}Rb we performed a search for additional strong transitions observed in the decay of the 5^- isomer. In particular, a 2648-keV, 4^- level is very strongly populated in the 5^- isomer decay with depopulating transitions of 554.35 keV ($I_\gamma = 74$) and 827.83 keV ($I_\gamma = 24.9$), relative to $I_\gamma = 100$ for the 776.5-keV transition. We find no evidence for either the 554- or 828-keV transitions in either the singles or γ-γ data, providing additional support that only the decay of the ground state is observed in the present work.

Many additional new transitions and levels have been observed in the present work, as indicated in Table I. In total, we observe 50 new transitions as well as 12 new levels. The prior study of the β decay of ^{82}Rb observed 7 transitions that were not consistent with our present work. Those transitions are 467, 869, 1021, 1081, 1125, 1699, and 2242 keV. The 1021-keV transition previously seen is likely a sum peak from 511+511 annihilation lines. The other 6 have not been observed in the present work and, therefore, have been dismissed. The 869-, 1021-, and 1699-keV transitions were previously considered tentative.

B. Angular correlation analysis

In cases where statistics were sufficient, the spin for a level was determined using angular correlations analysis. In all the analyzed cases, a gate was placed on a known $2^+ \rightarrow 0^+$ transition and the intensity of the populating transition determined for all angle groupings. The 0-2-0 cascade exhibits a unique and distinct pattern, allowing for unambiguous identification of $J = 0$ states. The $J = 0$ spin assignments for the 1488- and 2172-keV levels were confirmed using the 711-776.5 and the 1395-776.5 cascade, respectively. The angular correlation analysis for the 2172-keV level is shown in Fig. 6(a). To illustrate the striking difference between the 0-2-0 pattern and other J^π cascades, the angular correlation analysis for the 1180-776.5-keV cascade (stars) and the theoretical predictions for a 2-2-0 sequence with $\delta = -0.52$ (dotted line) are included in Fig. 6(c).

A number of additional levels were found to have $W(\theta)$ patterns consistent with 0-2-0 sequences. These include the 2450-, 3187-, 3234-, 3565-, and 3717-keV levels which were obtained using the cascades 975-776.5, 2411-776.5, 2458-776.5, 1608-1957, and 2941-776.5, respectively. The angular correlations for these cascades are given in Fig. 6. Each of these levels were previously assigned as $J = 0,1,2$.

The 1957-keV level was tentatively assigned (2^+) [16]. Angular correlation analysis of the 1180-776.5 cascade confirmed a $J = 2$ assignment and yielded a mixing ratio for the 1180-keV transtion of $\delta = -0.52(16)$. A level at 2480 keV was previously assigned as a $1^+,2^+$ state [16]. A spin of $J = 2$ was determined from the analysis of the 1704-776 cascade. The large mixing ratio of $\delta = 1.03(10)$ obtained for

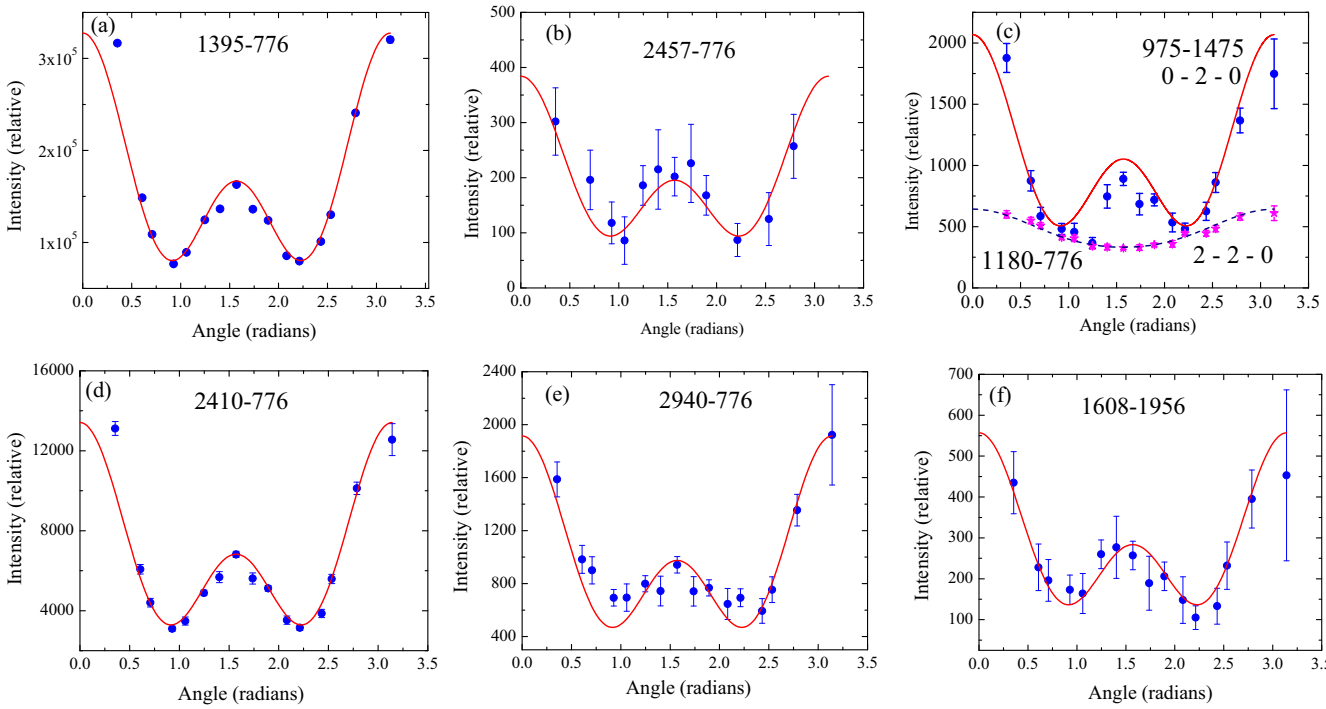

FIG. 6. Angular correlation analysis of confirmed and newly identified $0^+ \rightarrow 2^+ \rightarrow 0^+$ cascade transitions in ^{82}Kr. Solid circles give the measured intensity as a function of angle between detectors while solid lines are the theoretical predictions for a 0-2-0 sequence. Numbers in each panel give the cascade energies, in keV. In panel (c), the angular correlation of the 1180-776.5 cascade (stars) is given along with the theoretical predictions for a 2-2-0 sequence with $\delta = -0.52$ (dotted line).

the 1703.5-keV $2 \rightarrow 2$ transition suggests $M1 + E2$ character, and thus a $J^\pi = 2^+$ is assigned to the 2480-keV level. The same analysis was done for the 2656-keV level using the 1880-776.5 cascade. This level was previously assigned as a $1,2^{(+)}$. The cascade confirmed a spin of $J = 2$ with a mixing ratio of $-0.71(21)$ for the 1880-keV transition. This also suggests the transition has $M1 + E2$ character. The 2945-keV level was previously assigned as a $(2)^+$ state. Using the same analysis, it was confirmed as a $J = 2$ state from the analysis of the 2168-776.5 cascade. The mixing ratio for the 2168-keV transition was determined to be <0.06. While parity can not directly be determined from this ratio, the observed transition to the ground state favors a $J^\pi = 2^+$ assignment.

V. DISCUSSION

The precise and consistent measurements of the absolute intensity [10–12] of the 776-keV transition provide a sound basis on which to normalize the decay scheme and deduce β-feeding intensities. The ground-state β-feeding intensity is paramount for the use of this isotope in PET imaging, as the large ground-state to ground-state β transition is the dominant source of positrons. The branch has not been measured directly and is deduced by first normalizing the entire decay scheme to the 776-keV absolute intensity and then applying conservation of flux with

$$100 = \sum I(\gamma + ce)(\text{to g.s.}) + I(ec + \beta)(\text{to g.s.}). \quad (1)$$

In the prior evaluated data on ^{82}Rb decay [16], the total γ-ray flux to the ground state was calculated to be 15.23 (17)%, yielding a ground-state to ground-state β-feeding intensity of 84.77 (17)%. The ratio of electron capture to positron emission can be calculated [23] and due to the large Q value of the decay, the 84.77% ground-state branch decomposes into 81.76% positron emission and 3.01% electron capture decay. The previous value for $\sum I(\gamma+\text{ce})$ (to gs) was derived using a normalization factor of 0.1508(16), obtained by taking a weighted average of the absolute intensity measurements of Refs. [10] and [11]. In the present work, we also incorporate the newer measurement of Ref. [12] to obtain a normalization factor of 0.1506(15). Applying this normalization factor to the newly measured decay scheme yields a total γ-ray flux to the ground state of 15.22(15)% with a corresponding ground-state to ground-state feeding intensity of 84.78 (15)%. Despite the many changes to the ^{82}Rb decay scheme identified in the present work and consequent changes to the γ-ray feeding pattern, it turns out that the total ground-state to ground-state feeding intensity remains almost unchanged, and similarly the positron to electron capture ratio. Inspection of Fig. 2 and Table I reveal that a single new ground-state decay was observed from a 2993-keV level, and the relative intensity was only $1.7(2) \times 10^{-5}$ that of the 776-keV transition, making a negligible contribution.

A similar finding comes when calculating the energy-weighted mean γ-ray and positron kinetic energy, which dictate the overall dose received by the patient. This is determined by summing the product of the energy multiplied by the intensity for each radiation emitted from the source. The lepton energies and intensities can be derived from the observed energy levels, the Q value of 4403(3) keV [22], and

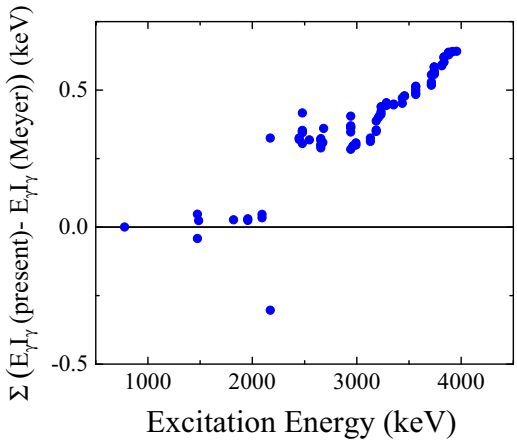

FIG. 7. Difference between the energy-weighted sum from the present work compared with that of Ref. [9], plotted as a function of excitation energy in ^{82}Kr.

the γ-ray decay pattern. Table I shows considerable difference between the current work and Ref. [9], with the number of γ-ray transitions now known more than doubled. Fortunately for dosimetry, the new transitions are extremely weak and so contribute little to the intensity-weighted energy sum. Figure 7 shows the difference between the intensity-weighted sum of γ rays from Table I from the present work and Ref. [9]. The two experiments are very consistent below 2 MeV, but the many new transitions from high-lying states eventually make a small contribution in increasing the energy-weighted sum. In calculating the total dose, the contribution from γ rays from excited states has to be folded with the dominant contribution of γ rays from the positron annihilation. Most of the new states are populated by electron capture of low intensity and therefore contribute little to the intensity-weighted γ dose. Using the results of the current work, we obtain an average γ-ray energy of 1108.1(16) keV and an average positron energy of 1411 keV. This is less than 1 keV different from the values one would obtain from the decay scheme of Ref. [9].

.

VI. CONCLUSIONS

The decay of the important cardiac PET imaging isotope ^{82}Rb was studied with the Gammasphere array. The new high-statistics data significantly revise the level scheme, and include the observations of 12 new levels and 50 new transitions. Despite the many changes to the level scheme, the dosimetry properties of ^{82}Rb remain almost identical to the current literature values. The low effective dose received by patients reported in Ref. [5] does not appear to be due to any deficiency in the actual nuclear decay scheme and so must be attributed to biological effects. We believe this result is somewhat fortuitous, due to a cancellation between renormalization and the contribution of the new γ rays, and other medical isotopes may show considerable modification to their dosimetric properties when contemporary spectroscopy is performed.

ACKNOWLEDGMENTS

DOE Isotope Program is acknowledged for funding ST5001030. Work was supported by the US DOE under Grant No. DE-FG02-94ER40848 and Contracts No. DE-AC02-98CH10946 and No. DE-AC02-06CH11357 and by the DOE Office of Science, Office of Workforce Development for Teachers and Scientists (WDTS), under the Science Undergraduate Laboratory Internships Program (SULI). This research used resources of Argonne National Laboratory's ATLAS facility, which is a DOE office of Science User Facility.

[1] K. Yoshinaga, R. Klein, and N. Tamaki, J. Cardiol. **55**, 163 (2010).
[2] B. A. McArdle, T. F. Dowsley, R. A. deKemp, G. A. Wells, and R. S. Beanlands, J. Am. Coll. Cardiol. **60**, 1828 (2012).
[3] T. Xie, C. Lee, W. Bolch, and H. Zaidi, Med. Phys. **42**, 2955 (2015).
[4] S. Senthamizhchelvan, P. E. Bravo, C. Esaias, M. A. Lodge, J. Merrill, R. F. Hobbs, G. Sgouros, and F. M. Bengel, J. Nucl. Med. **51**, 1592 (2010).
[5] C. R. R. N. Hunter, J. Hill, M. C. Ziadi, R. S. B. Beanlands, and R. A. deKemp, Eur. J. Nucl. Mol. Imaging **42**, 1032 (2015).
[6] ICRP Publication 80, Ann ICRP **28**, 1 (1998).
[7] M. G. Stabin, R. B. Sparks, and E. Crowe, J. Nucl. Med. **46**, 1023 (2005).
[8] J. C. Hardy, L. C. Carraz, B. Jonson, and P. G. Hansen, Phys. Lett. B **71**, 307 (1977).
[9] R. A. Meyer, J. F. Wild, K. Eskola, M. E. Leino, S. Väisälä, K. Forssten, U. Kaup, and A. Gelberg, Phys. Rev. C **27**, 2217 (1983).
[10] S. M. Judge, M. J. Woods, S. L. Walters, and K. R. Butler, Appl. Radiat. Isot. **38**, 185 (1987).
[11] D. D. Hoppes, B. M. Coursey, F. J. Schima, and D. Yang, Appl. Radiat. Isot. **38**, 195 (1987).
[12] C. J. Gross *et al.*, Phys. Rev. C **85**, 024319 (2012).
[13] K. E. Thomas, Appl. Rad. Isot. **38**, 175 (1987).
[14] L. F. Mausner, T. Prach, and S. C. S. Srivastava, Appl. Rad. Isot. **38**, 181 (1987).
[15] I-Y. Lee, Prog. Part. Nucl. Phys. **28**, 473 (1992).
[16] J. K. Tuli, Nucl. Data Sheets **98**, 209 (2003).
[17] http://www.phy.anl.gov/gammasphere/doc/index.html.
[18] D. C. Radford, Nucl. Instrum. Methods Phys. Res., Sect. A **361**, 297 (1995).
[19] W. D. Kulp *et al.*, Phys. Rev. C **76**, 034319 (2007).
[20] B. Singh and J. C. Roediger, Nucl. Data Sheets **111**, 2081 (2010).
[21] H. Junde, H. Su, and Y. Dong, Nucl. Data Sheets **112**, 1513 (2011).
[22] M. Wang, G. Audi, A. H. Wapstra, F. G. Kondev, M. MacCormick, X. Xu, and B. Pfeiffer, Chin. Phys. C **36**, 1603 (2012).
[23] N. B. Grove and M. J. Martin, Nucl. Data Tables A **10**, 205 (1971).